Advanced echocardiography in characterization and management of patients with secondary mitral regurgitation

Namazi, F.

Chapter five

Prognostic Implications of Mitral Valve Geometry in Patients with Secondary Mitral Regurgitation: The COAPT Trial

Farnaz Namazi, Victoria Delgado, Stephan Milhorini Pio, Nina Ajmone Marsan, Federico M. Asch, Neil J. Weissman, Zhipeng Zhou, Bjorn Redfors, JoAnn Lindenfeld, William T. Abraham, Michael J. Mack, Gregg W Stone, Jeroen J. Bax.

European Heart Journal - Cardiovascular Imaging, 2021

Abstract

Aims

The impact of mitral valve geometry on outcomes after MitraClip treatment in secondary MR has not been examined. We therefore sought to evaluate the association between mitral valve geometry and outcomes of patients with heart failure (HF) and secondary mitral regurgitation (MR) treated with guideline-directed medical therapy (GDMT) and MitraClip.

Methods and Results

Mitral valve geometry was assessed from the baseline echocardiograms in 614 patients from the COAPT trial. The primary endpoint for the present study was the composite of all-cause mortality or HF hospitalization (HFH) within 2 years. Effect of treatment arm (MitraClip plus maximally-tolerated GDMT versus GDMT alone) on outcomes according to baseline variables was assessed.

Among 29 baseline mitral valve echocardiographic parameters, increasing antero-posterior mitral annular diameter was the only independent predictor of the composite endpoint of all-cause mortality or HFH (adjusted hazard ratio (aHR) per cm 1.49; p=0.04). The effective regurgitant orifice area (EROA) was independently associated with all-cause mortality alone (aHR per cm^2 2.97; p=0.04) but not with HFH, whereas increasing anteroposterior mitral annular diameter was independently associated with HFH alone (aHR per cm 1.85; p=0.005) but not all-cause mortality. Other mitral valve morphologic parameters were unrelated to outcomes. MitraClip reduced HFH and mortality independent of anteroposterior mitral annular diameter and EROA ($P_{interaction}$= 0.77 and 0.27 respectively).

Conclusion

In patients with HF and severe secondary MR, a large anteroposterior mitral annular diameter and greater EROA were the strongest echocardiographic predictors of HFH and death in patients treated with GDMT alone and with the MitraClip.

Introduction

In prior studies of patients with heart failure (HF) and secondary mitral regurgitation (MR), quantification of MR severity, indices of left ventricular (LV) function and remodeling, and clinical symptoms have been the principal parameters used to assess prognosis and select the most appropriate therapy (1,2). Guideline-directed medical therapy (GDMT) for HF is foundational for all patients and may reduce MR by decreasing LV dimensions (3,4). Cardiac resynchronization therapy has been shown to further reduce MR in some patients with HF (5,6). When surgical coronary revascularization is needed, concomitant mitral annuloplasty is often performed (1,2). However, recurrent MR after annuloplasty is not uncommon and has been associated with increased mortality and morbidity (7,8). In patients with non-ischemic cardiomyopathy and severe secondary MR, surgical mitral valve repair has also been associated with high operative risk and its variable durability (7,8). Specific mitral valve geometric abnormalities and the extent of LV remodeling have been associated with recurrence of MR after surgical mitral valve repair and reduced survival (7-10).

More recently, transcatheter mitral valve repair (TMVr) has been introduced for the treatment of HF patients with severe secondary MR, the most widely studied of which is transcatheter mitral leaflet edge-to-edge approximation with the MitraClip. A decade ago, numerous mitral valve anatomic criteria were established that predicted success (or failure) of the MitraClip (11,12). However, these studies were performed before widespread usage of this device. Procedural success rates have greatly improved within the last decade, and in the present era less is known about the mitral valve anatomic parameters that predict procedural success and long-term outcomes with the MitraClip (and may vary in primary and secondary MR). In this regard, disparate outcomes of HF patients enrolled in the Cardiovascular Outcomes Assessment of the MitraClip Percutaneous Therapy for Heart Failure Patients With Functional Mitral Regurgitation (COAPT) (13) and the Multicentre Study of Percutaneous Mitral Valve Repair MitraClip Device in Patients With Severe Secondary Mitral Regurgitation (MITRA-FR) (14) trials were reported, which has most often been attributed to inter-study differences in LV dilation, LV function and MR severity. However, a detailed analysis of mitral valve geometry and its interplay with LV remodeling and MR severity in determining the clinical outcomes of patients randomized to MItraClip plus GDMT versus GDMT alone has not been performed in either study. Accordingly, in the present sub-study from the COAPT trial, we assessed the association between various geometric mitral valve parameters and clinical outcomes. We hypothesized that more advanced mitral valve apparatus deformation would be associated with worse outcomes independent of

treatment arm, and that MitraClip treatment would mitigate the impact from these prognostic risk factors.

Methods

Study design and patient population

Details concerning the COAPT study design and patient population have been published previously (13,15). In brief, HF patients with ischemic or non-ischemic cardiomyopathy and with moderate-to-severe (grade 3+) or severe (grade 4+) secondary MR who remained symptomatic despite the use of maximally-tolerated GDMT were enrolled. Patients were randomized to TMVr using the MitraClip device (Abbott Vascular, Santa Clara, CA) plus GDMT or GDMT alone. Procedural data have been published previously (13). The primary endpoint of the present analysis was the composite of all-cause death or heart failure hospitalization (HFH) at 24-month follow-up. Secondary endpoints included all-cause mortality and HFH alone. The protocol was registered on ClinicalTrials.gov (#NCT01626079) and was approved by the investigational board of each participating center. All patients provided written informed consent. The sponsor participated in site selection and management and in data analysis. The principal investigators had unrestricted access to the data, wrote the manuscript, and vouch for the accuracy and completeness of the data and analyses and for the fidelity of the trial to the protocol.

Echocardiography

Baseline conventional echocardiographic measurements were performed by an independent echocardiographic core laboratory (MedStar Health Research Institute, Washington DC) and have been published previously (13,16). Left and right ventricular dimensions and function were measured according to current recommendations (17,18). MR was quantified using a multiparametric algorithm based on recommendations from the American Society of Echocardiography (13,19). Tricuspid regurgitation (TR) was also graded based on a multiparametric approach consisting of qualitative and semiquantitative parameters (19).

For the present post hoc analysis, mitral valve geometric analysis was performed using commercially available software for offline analysis (TomTec-Arena, version 20.18, 2017). Table 1 and Figures 1 and 2 summarize the mitral valve geometrical variables measured (9,10,20-22). All measurements were done on transthoracic echocardiograph. The measurements were performed per multiple beats if atrial fibrillation was present. The

diameters of the mitral valve annulus were measured in the anteroposterior direction from the parasternal long-axis view and in the intercommissural direction from the apical 2-chamber view. Mitral valve tethering was assessed measuring the distance between the coaptation point to septum, tenting height (the distance between the coaptation point of the mitral valve leaflets and the mitral valve annular plane) and tenting area (the area enclosed by the mitral valve leaflets and the mitral annular plane). The length of the anterior and posterior mitral valve leaflets were measured in mid-diastole on the parasternal long-axis view. The maximal tethering location was determined according to the scallops of the posterior mitral leaflet. The distance from the posterior papillary muscle to the mitral annulus was measured in the apical 4- and 2-chamber views while the distance from the anterior papillary muscle to the mitral annulus was measured in the apical 2-chamber view. The mitral posterior leaflet angle and the basal and distal anterior leaflet angles were measured on the apical long-axis view.

Statistical analysis

Categorical data are presented as frequencies and were compared by Chi-square test or Fisher's exact test, as appropriate. Continuous variables are presented as means and standard deviation or median [Q1, Q3] and were compared by Student's t-test or Wilcoxon Rank Sum test. The independent association between the various clinical and echocardiographic parameters with the occurrence of the endpoint was assessed with univariate and multivariable Cox proportional hazards regression analysis. The relative effect of treatment vs. control arms on the risk of the endpoints associated with clinical and echocardiographic variables was assessed by formal interaction testing. Statistical analyses were performed with SAS version 9.4 (SAS Institute, Cary, NC).

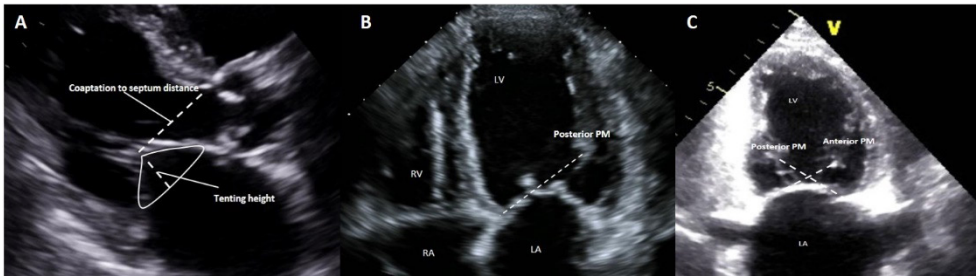

Figure 1. Examples of mitral valve geometry measurements on two-dimensional transthoracic echocardiography.

Panel A shows the parasternal long-axis view, demonstrating the measurements of coaptation to septum distance, tenting height and tenting area (the area enclosed by white lines). Panel B shows the apical 4-chamber view, demonstrating the measurement of posterior papillary muscle

tethering length (the white dashed line from the posterior papillary muscle to the contralateral mitral valve annulus). Panel C shows the apical 2-chamber view, demonstrating the posterior papillary muscle to the mitral valve annulus distance (the white dashed line from the posterior papillary muscle to the contralateral mitral valve annulus) and the anterior papillary muscle to the mitral valve annulus distance (the white dashed line from the anterior PM to the contralateral mitral valve annulus).

Table 1. Summary of mitral valve geometry measurements using two-dimensional transthoracic echocardiography.

Parameter	Definition	TTE view	Timing on TTE
Anterior-posterior mitral annulus diameter	The distance between the anterior point and posterior point of the mitral annulus	Parasternal long-axis	End-diastole
Intercommissural mitral annulus diameter	The distance from commissure to commissure of the mitral annulus	Apical 2-chamber view	End-diastole
Anterior and posterior mitral valve leaflet length	The length of the mitral valve leaflet measured from the hinge point of the leaflet to the leaflet tip	Parasternal long-axis	Diastole, maximum extension of leaflets
Coaptation to septum distance	The distance between the coaptation point of the mitral valve leaflets and the septum at the hinge point of the aortic valve cusps	Parasternal long-axis	Mid-systole
Tenting height	The distance between the coaptation point of the mitral valve leaflets and the mitral annular plane	Parasternal long-axis	Mid-systole
Tenting area	The area enclosed by the mitral valve leaflets and the mitral annular plane	Parasternal long-axis	Mid-systole
Anterior- and posterior papillary muscle to mitral valve annulus distance	The distance between the PM tips to the contralateral mitral annulus, providing an estimation of PM displacement	Apical 2-chamber view (if not visible, measured on apical 4-chamber view)	Mid-systole
Basal mitral anterior leaflet angle	The angle between the basal anterior leaflet and mitral annulus (traced from mitral annular plane to the bending point of the anterior mitral valve leaflet)	Apical 4-chamber view	Mid-systole
Distal mitral anterior leaflet angle	The angle between the anterior leaflet and mitral valve annulus (traced from mitral annular plane to the bending point of the anterior mitral valve leaflet)	Apical 4-chamber view	Mid-systole
Posterior mitral leaflet angle	The angle between the posterior leaflet and mitral valve annulus (traced from mitral annular plane to the tip of the posterior mitral valve leaflet)	Apical 4-chamber view	Mid-systole

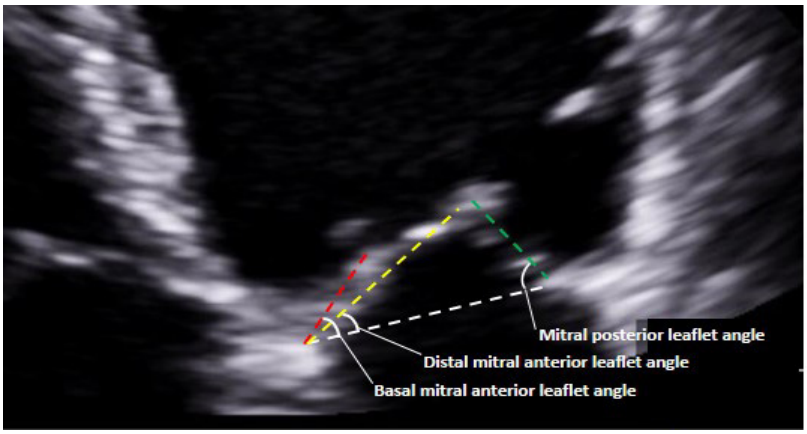

Figure 2. Example of mitral valve angle quantification on echocardiography.
The white dashed line represents the mitral valve annular plane. The red dashed line represents the line from the mitral valve annulus to the bending point of the anterior mitral leaflet, defining the basal mitral anterior leaflet angle (ALA_{base}). The yellow dashed line represents the line from the mitral valve annulus to the tip of the anterior mitral leaflet, defining the distal mitral anterior leaflet angle (ALA_{dist}). The green dashed line represents the line from the mitral valve annulus to the tip of the posterior mitral leaflet, defining the posterior mitral leaflet angle (PLA).

Results

Baseline clinical characteristics have been previously reported (13) and are summarized in Supplemental Appendix Table 1. The echocardiographic characteristics including the mitral valve geometry analysis are outlined in Table 2. The mean intercommissural (3.56 ± 0.43 cm) and anteroposterior (3.26 ± 0.39 cm) mitral annulus diameters were comparable demonstrating a circular rather than an elliptical shape of the mitral annulus. Significant tethering of the mitral valve leaflets was observed as indicated by the large distance between the point of coaptation and the interventricular septum, the increased tenting height/area and the increased posterior leaflet angle. Leaflet tethering was most frequently observed at the central level of the posterior mitral leaflet (P2). Intraobserver reproducibility of all the mitral valve echocardiographic measurements was tested in a randomly selected sample of 20 cases. Agreement was very good or excellent for all mitral valve measurements (intraclass coefficient [ICC] >0.7), except for the length of the anterior and posterior mitral valve leaflets (ICC 0.5; 95% CI 0.24 to 0.78 and ICC 0.57; 95% CI 0.15 to 0.74, respectively), and the anterior papillary muscle to mitral valve annulus distance (ICC 0.26; 95% CI -0.14 to 0.58). As previously described, patients had severe MR with a mean effective regurgitant orifice

area (EROA) of 0.41 cm^2, regurgitant volume of 26.8 ml/beat and regurgitant fraction of 36.4%. Moderately severe LV remodeling was observed with a mean LV end-systolic diameter of 5.3 cm and end-diastolic diameter of 6.2 cm. Mean LV end-systolic volume was 134.7 ml and end-diastolic volume 192.8 ml resulting in a mean LV ejection fraction of 31.3%. Mean right ventricular fractional area change was impaired with a mean value of 32.0%. The mean right ventricular systolic pressure (RVSP) was increased (44.3 ± 13.7 mmHg) and the majority of patients had mild tricuspid regurgitation.

Impact of mitral valve geometry and cardiac structure and function on MR reduction

Among 274 patients who were randomized to and treated with the MitraClip, at 30 days grade 0 or 1+ MR was present in 199 patients (72.6%), grade 2+ MR was present in 54 patients (19.7%) and grade 3+ or 4+ MR was present in 21 patients (7.7%). As shown in Table 3, patients with 3+ or 4+ MR at 30 days post-MitraClip had a significantly larger mitral posterior leaflet angle at baseline than those with £2+ MR. The tethering location was also significantly different between the groups; specifically, while mitral leaflet tethering at P3 was uncommon (7 patients), 3 of these patients (42.9%) had ^{3}3+ MR at 30 days after MitraClip. No other significant differences were observed in mitral valve geometry at baseline according to MR grade 30 days after MitraClip. In terms of conventional echocardiographic characteristics, patients with grade 3+ or 4+ MR 30-days after MitraClip had more severe MR at baseline, larger total stroke volume, larger LV end-diastolic volume index and higher RVSPs.

Table 2. Echocardiographic characteristics at baseline for the total population.

Mitral valve geometrical measurements	
Intercommissural mitral valve annulus diameter (cm)	3.56 ± 0.43 (577)
Anteroposterior mitral valve annulus diameter (cm)	3.26 ± 0.39 (575)
Coaptation to septum distance (cm)	4.04 ± 0.46 (559)
Tenting height (mm)	9.9 ± 2.4 (569)
Tenting area (cm^2)	2.16 ± 0.68 (568)
Anterior mitral valve leaflet length (cm)	2.25 ± 0.37 (551)
Posterior mitral valve leaflet length (cm)	1.35 ± 0.24 (472)
Tethering location, n/N (%)	
None	21/465 (4.5)
P1	60/465 (12.9)
P1-P2	109/465 (23.4)
P2	183/465 (39.4)
P2-P3	68/465 (14.6)
P3	22/465 (4.7)
All	2/465 (0.4)

Mitral valve geometrical measurements	
Posterior papillary muscle to annulus distance (cm; 4CH view)	4.19 ± 0.59 (275)
Posterior papillary muscle to annulus distance (cm; 2CH view)	4.02 ± 0.58 (256)
Anterior papillary muscle to annulus distance (cm)	3.81 ± 0.57 (226)
Basal mitral anterior leaflet angle (°)	32 ± 7 (244)
Distal mitral anterior leaflet angle (°)	19 ± 6 (516)
Mitral posterior leaflet angle (°)	38 ± 9 (501)
Mitral valve regurgitation quantification	
Mitral regurgitation, n/N (%)	
(3+) Moderate to severe	320/613 (52.2)
(4+) Severe	293/613 (47.8)
Effective regurgitant orifice area (cm^2)	0.41 ± 0.15 (591)
Regurgitant volume (mL/beat)	26.8 ± 16.2 (260)
Regurgitant fraction (%)	36.4 ± 14.5 (259)
Left ventricular measures	
LV end-systolic diameter (cm)	5.3 ± 0.9 (607)
LV end-diastolic diameter (cm)	6.2 ± 0.7 (608)
LV end-systolic volume (mL)	134.7 ± 58.2 (574)
LV end-diastolic volume (mL)	192.8 ± 71.1 (574)
Total stroke volume (mL)	58.0 ± 22.6 (574)
LV end-systolic volume index (mL/m^2)	71.1 ± 29.1 (567)
LV end-diastolic volume index (mL/m^2)	101.4 ± 34.4 (567)
LV ejection fraction (%)	31.3 ± 9.3 (575)
LV sphericity index*	0.65 ± 0.1 (524)
Right ventricular measures	
RV fractional area change (%)	32.04 ± 8.98 (417)
RV systolic pressure (mmHg)	44.3 ± 13.7 (528)
Tricuspid regurgitation, n/N (%)	
(0) None	12/599 (2.0)
(1+) Mild	489/599 (81.6)
(2+) Moderate	92/599 (15.4)
(3+) Moderate to Severe	5/599 (0.8)
(4+) Severe	1/599 (0.2)
Left atrial measures	
Left atrial volume (mL)	91.4 ± 40.8 (595)

Data presented as mean ± SD (n) or n/N (%). CH = chamber; LV = left ventricular; RV = right ventricular; MV = mitral valve; PM = papillary muscle. *LV sphericity index was defined as LV short axis / LV long axis. Both axis measurements were taken in 4-chamber view.

Table 3. Impact of Baseline Echocardiographic Parameters on Post-MitraClip Severity of Mitral Regurgitation at 30 Days.

	MR grade at 30 days			
	Grade 0 or 1+	**Grade 2+**	**Grade 3+ or 4+**	**P-value**
Mitral valve geometrical measurements				
Intercommissural mitral valve annulus diameter (cm)	3.56 ± 0.42 (188)	3.53 ± 0.34 (49)	3.66 ± 0.41 (18)	0.50
Anteroposterior mitral valve annulus diameter (cm)	3.26 ± 0.40 (188)	3.24 ± 0.30 (48)	3.36 ± 0.34 (20)	0.44
Coaptation to septum distance (cm)	4.07 ± 0.44 (182)	4.01 ± 0.44 (47)	4.08 ± 0.38 (20)	0.68
Tenting height (mm)	9.8 ± 2.5 (186)	10.2 ± 2.5 (48)	9.5 ± 1.5 (20)	0.48
Tenting area (cm^2)	2.13 ± 0.71 (186)	2.16 ± 0.69 (48)	2.26 ± 0.59 (20)	0.71
Anterior mitral valve leaflet length (cm)	2.26 ± 0.34 (174)	2.25 ± 0.43 (47)	2.37 ± 0.37 (19)	0.47
Posterior mitral valve leaflet length (cm)	1.34 ± 0.25 (141)	1.34 ± 0.23 (39)	1.29 ± 0.17 (19)	0.70
Tethering location, n/N (%)				**0.05**
None	5/149 (3.4)	1/38 (2.6)	0/17 (0.0)	
P1	18/149 (12.1)	2/38 (5.3)	2/17 (11.8)	
P1-P2	43/149 (28.9)	10/38 (26.3)	3/17 (17.6)	
P2	61/149 (40.9)	16/38 (42.1)	8/17 (47.1)	
P2-P3	18/149 (12.1)	8/38 (21.1)	1/17 (5.9)	
P3	4/149 (2.7)	0/38 (0.0)	3/17 (17.6)	
All	0/149 (0.0)	1/38 (2.6)	0/17 (0.0)	
Posterior papillary muscle to annulus distance (cm; 4CH view)	4.17 ± 0.61 (95)	4.25 ± 0.58 (27)	4.61 ± 0.50 (10)	0.08
Posterior papillary muscle to annulus distance (cm; 2CH view)	4.07 ± 0.55 (83)	3.88 ± 0.49 (24)	3.91 ± 0.66 (12)	0.24
Anterior papillary muscle to annulus distance (cm)	3.84 ± 0.69 (77)	3.62 ± 0.50 (17)	4.02 ± 0.72 (7)	0.34
Basal mitral anterior leaflet angle (°)	31 ± 6 (81)	33 ± 6 (22)	28 ± 8 (9)	0.13
Distal mitral anterior leaflet angle (°)	18 ± 6 (164)	20 ± 6 (47)	20 ± 7 (17)	0.11
Mitral posterior leaflet angle (°)	37 ± 9 (161)	41 ± 8 (45)	41 ± 11 (14)	**0.04**
Mitral valve regurgitation quantification				
Mitral regurgitation, n/N (%)				**0.0001**
(3+) Moderate to severe	116/199 (58.3)	19/54 (35.2)	4/21 (19.0)	
(4+) Severe	83/199 (41.7)	35/54 (64.8)	17/21 (81.0)	

	MR grade at 30 days			
	Grade 0 or 1+	**Grade 2+**	**Grade 3+ or 4+**	**P-value**
Effective regurgitant orifice area (cm^2)	0.40 ± 0.16 (189)	0.43 ± 0.13 (53)	0.45 ± 0.15 (21)	0.35
Regurgitant volume (mL/beat)	28.2 ± 14.7 (78)	28.2 ± 23.2 (26)	33.6 ± 19.3 (14)	0.56
Regurgitant fraction (%)	37.2 ± 12.9 (77)	38.5 ± 15.1 (26)	40.9 ± 16.9 (14)	0.65
Left ventricular measures				
LV end-systolic diameter (cm)	5.3 ± 0.9 (199)	5.3 ± 0.8 (53)	5.2 ± 0.7 (21)	0.89
LV end-diastolic diameter (cm)	6.2 ± 0.7 (199)	6.2 ± 0.8 (53)	6.3 ± 0.6 (21)	0.84
LV end-systolic volume (mL)	133.2 ± 57.5 (188)	139.5 ± 57.1 (50)	148.8 ± 53.7 (19)	0.46
LV end-diastolic volume (mL)	191.0 ± 69.4 (188)	199.1 ± 70.6 (50)	224.4 ± 67.7 (19)	0.12
Total stroke volume (mL)	57.7 ± 20.5 (188)	59.5 ± 24.2 (50)	75.6 ± 27.0 (19)	**0.003**
LV end-systolic volume index (mL/m^2)	69.1 ± 27.6 (188)	76.0 ± 32.0 (48)	78.1 ± 28.3 (19)	0.18
LV end-diastolic volume index (mL/m^2)	99.1 ± 32.5 (188)	107.8 ± 38.7 (48)	117.0 ± 32.1 (19)	**0.04**
LV ejection fraction (%)	31.4 ± 8.9 (188)	31.1 ± 9.6 (50)	34.4 ± 9.2 (19)	0.35
Right ventricular measures				
RV fractional area change (%)	32.43 ± 8.24 (131)	30.63 ± 8.87 (40)	34.09 ± 8.06 (14)	0.33
RV systolic pressure (mmHg)	42.2 ± 13.4 (162)	47.0 ± 13.2 (49)	47.9 ± 15.5 (18)	**0.04**
Tricuspid regurgitation, n/N (%)				0.79
(0) None	4/197 (2.0)	3/54 (5.6)	1/20 (5.0)	
(1+) Mild	168/197 (85.3)	45/54 (83.3)	16/20 (80.0)	
(2+) Moderate	23/197 (11.7)	6/54 (11.1)	3/20 (15.0)	
(3+) Moderate to Severe	2/197 (1.0)	0/54 (0.0)	0/20 (0.0)	
(4+) Severe	0/197 (0)	0/54 (0.0)	0/20 (0.0)	

Data presented as mean ± SD (n) or n/N (%). CH = chamber; LV = left ventricular; RV = right ventricular; MV = mitral valve; PM = papillary muscl

Impact of mitral valve geometry on all-cause death or HFH at 24 months

In the entire patient population, larger baseline anteroposterior and intercommissural mitral annular diameters were the only mitral valve anatomic parameters that were significantly associated with the composite risk of death or HFH at 24 months (Table 4). Severe MR, moderate or greater TR and increasing mitral EROA and RVSP were

also significantly associated with the primary endpoint. By multivariable analysis, the baseline anteroposterior mitral annulus diameter was the only echocardiographic variable independently associated with the primary endpoint. Of note, baseline mitral EROA was not an independent predictor of the 2-year composite clinical outcome. A history of atrial fibrillation or flutter, New York Heart Association (NYHA) class and baseline BNP plasma levels were also independently associated with occurrence of the primary composite endpoint within 2 years.

Table 4. Univariable and multivariable predictors of the composite outcome of all-cause mortality or heart failure hospitalization at 2-year follow-up.

	Univariable analysis		Multivariable analysis	
Variable	**HR (95% CI)**	**p-Value**	**HR (95% CI)**	**p-Value**
Echocardiographic parameters at baseline				
Anterior-posterior mitral annulus diameter (per cm)	**1.55 (1.16 - 2.08)**	**0.003**	**1.49 (1.02 - 2.19)**	**0.04**
Intercommisural mitral annulus diameter (per cm)	**1.38 (1.07 - 1.80)**	**0.01**		
Anterior mitral valve leaflet length (per cm)	1.30 (0.95 - 1.78)	0.10		
Posterior mitral valve leaflet length (per cm)	1.09 (0.65 - 1.83)	0.75		
Coaptation to septum distance (per cm)	1.00 (0.77 - 1.28)	0.97		
Tenting height (per cm)	1.25 (0.79 - 1.98)	0.35		
Tenting area (per cm^2)	1.17 (1.00 - 1.38)	0.054	1.06 (0.85 - 1.33)	0.59
Anterior papillary muscle to MV annulus distance (per cm)	1.17 (0.87 - 1.58)	0.30		
Posterior papillary muscle to MV annulus distance (per cm)	1.22 (0.91 - 1.64)	0.18		
Basal mitral anterior leaflet angle (per degree)	1.01 (0.99 - 1.03)	0.42		
Distal mitral anterior leaflet angle (per degree)	1.01 (0.99 - 1.03)	0.34		
Posterior mitral leaflet angle (per degree)	1.00 (0.99 - 1.01)	0.76		
Tethering location	1.01 (0.91 - 1.12)	0.87		
Inferior basal/inferolateral LV aneurysm	1.10 (0.83 - 1.45)	0.50		
Posterior PM to annulus distance, 4CH (per cm)	0.98 (0.75 - 1.27)	0.86		
Left ventricular ejection fraction (per 10% increment)	0.90 (0.80 - 1.02)	0.09	0.91 (0.79 - 1.05)	0.21
Mitral regurgitation grade 4+ (vs. 3+)	**1.32 (1.07 - 1.64)**	**0.01**	0.93 (0.69 - 1.27)	0.13
Left ventricular end-diastolic dimension (per cm)	1.10 (0.95 - 1.27)	0.22		

	Univariable analysis		Multivariable analysis	
Variable	**HR (95% CI)**	**p-Value**	**HR (95% CI)**	**p-Value**
Right ventricular systolic pressure (per 10 mmHg)	1.20 (1.11 - 1.30)	<0.0001		
Tricuspid regurgitation severity ≥2+ (vs <2+)	**1.49 (1.13 - 1.95)**	**0.005**	1.29 (0.92 - 1.82)	0.15
Left ventricular end-diastolic volume (per 100 mL)	1.08 (0.92 - 1.26)	0.36		
Effective regurgitant orifice area, by PISA (per 1 cm^2)	**2.48 (1.29 - 4.79)**	**0.007**	1.72 (0.68 - 4.37)	0.25
Clinical variables at baseline				
Age (per 10 years)	**1.11 (1.01 - 1.23)**	**0.036**	0.99 (0.85 - 1.16)	0.94
MitraClip plus GDMT versus GDMT alone	**0.55 (0.44 - 0.69)**	**<0.0001**	**0.52 (0.40 - 0.67)**	**<0.0001**
Sex, male	1.21 (0.97 - 1.53)	0.10	1.17 (0.87 - 1.58)	0.29
Diabetes	1.24 (1.00 - 1.54)	0.053	1.26 (0.97 - 1.64)	0.08
Hypertension	1.17 (0.89 - 1.54)	0.26		
Hypercholesterolemia	1.09 (0.88 - 1.35)	0.44		
Previous myocardial infarction	1.13 (0.91 - 1.40)	0.27		
Previous percutaneous coronary intervention	1.11 (0.90 - 1.38)	0.33		
Previous stroke or transient ischemic attack	0.82 (0.61 - 1.11)	0.20		
Peripheral vascular disease	**1.33 (1.02 - 1.73)**	**0.04**	1.02 (0.73 - 1.42)	0.90
Chronic obstructive lung disease	1.22 (0.96 - 1.57)	0.11	1.08 (0.79 - 1.47)	0.65
History of atrial fibrillation or flutter	**1.33 (1.07 - 1.66)**	**0.01**	**1.44 (1.10 - 1.90)**	**0.009**
Body mass index (per 10 kg/m^2)	1.01 (0.83 - 1.22)	0.94		
Creatinine clearance (per 10 mL/min)	**0.93 (0.88 - 0.97)**	**0.001**	0.95 (0.89 - 1.01)	0.11
Anemia	1.26 (0.99 - 1.61)	0.06	1.22 (0.92 - 1.63)	0.17
Ischemic cardiomyopathy (vs. non-ischemic)	1.12 (0.89 - 1.39)	0.33		
New York Heart Association class IV (vs. II or III)	**2.25 (1.61 - 3.14)**	**<0.0001**	**1.90 (1.23 - 2.92)**	**0.004**
Heart failure hospitalization within the prior year	0.95 (0.76 - 1.18)	0.64		
Kansas City Cardiomyopathy Questionnaire score (per point)	**0.92 (0.88 - 0.97)**	**0.001**	0.97 (0.91 - 1.03)	0.35
Six-minute walk distance (per 50 meters)	**0.90 (0.86 - 0.94)**	**<0.0001**	0.95 (0.89 - 1.02)	0.13
B-type natriuretic peptide level (per 100 pg/mL)	**1.03 (1.02 - 1.03)**	**<0.0001**	**1.02 (1.01-1.03)**	**0.0005**

Death or HFH at 24 months occurred in 44.8% of patients randomized to MitraClip plus GDMT and in 66.1% of the patients randomized to GDMT alone (P<0.0001). MitraClip treatment was an independent predictor of a 48% reduction in the primary composite endpoint (P<0.0001; Table 4). By formal interaction testing, increasing anteroposterior mitral annular diameter was associated with a similar risk of the composite primary endpoint for both treatment arms (Central Illustration, Panel A). Similarly, no significant interactions between atrial fibrillation, NYHA class or BNP plasma levels and treatment arm were present for the primary composite outcome.

Impact of mitral valve geometry on all-cause death and heart failure hospitalization as separate outcomes

A larger mitral EROA was the only echocardiographic variable independently associated with an increased risk of all-cause mortality within 2 years (Supplemental Appendix Table 2). Other independent correlates of increasing mortality were creatinine clearance, 6-minute walk distance, BNP levels and EROA. MitraClip treatment was an independent predictor of a 38% reduction in 2-year mortality (P=0.003).There were no significant interactions noted between these variables and treatment arm on 24-month all-cause mortality (Central Illustration, Panel B).

Among the echocardiographic and mitral valve geometric variables, only the anteroposterior mitral annular diameter was independently associated with 2-year HFH (Supplemental Appendix Table 3). Other independent correlates of increasing mortality were history of atrial fibrillation or flutter, NYHA class, and BNP levels. MitraClip treatment was an independent predictor of a 57% reduction in 2-year HFH (P<0.001). There were no significant interactions noted between these variables and treatment arm on 24-month HFH (Central Illustration, Panel C).

Discussion

In the present sub-study from the COAPT trial, among HF patients with severe secondary MR, an increasing anteroposterior mitral annular diameter was associated with the 2-year composite endpoint of all-cause mortality or heart failure hospitalization, an association that was driven by an increasing risk of HFH more so than mortality. In contrast, baseline EROA was independently associated with the 2-year rate of all-cause mortality but not HFH. Treatment with MitraClip compared with GDMT alone reduced the relative 2-year risks of all-cause death, HFH and the composite of death or HFH consistently in all subgroups, including larger vs. smaller anteroposterior mitral annular

diameter and EROA. These findings demonstrate the complementary deleterious effects of a greater EROA (reflecting the severity of secondary MR) and an enlarged anteroposterior mitral annular diameter (reflecting long-standing volume overload). By reducing MR and having long-term favorable effects on LV remodeling (13,16), treatment of severe secondary MR with the MitraClip plus GDMT thus improves freedom from both death and HFH during long-term follow-up in selected patients with HF.

Central Illustration. Interactions between treatment arm and baseline mitral valve geometry and regurgitation severity for the 2-year composite endpoint of all-cause death or heart failure hospitalization (A), all-cause death alone (B) and heart failure hospitalization alone (C).

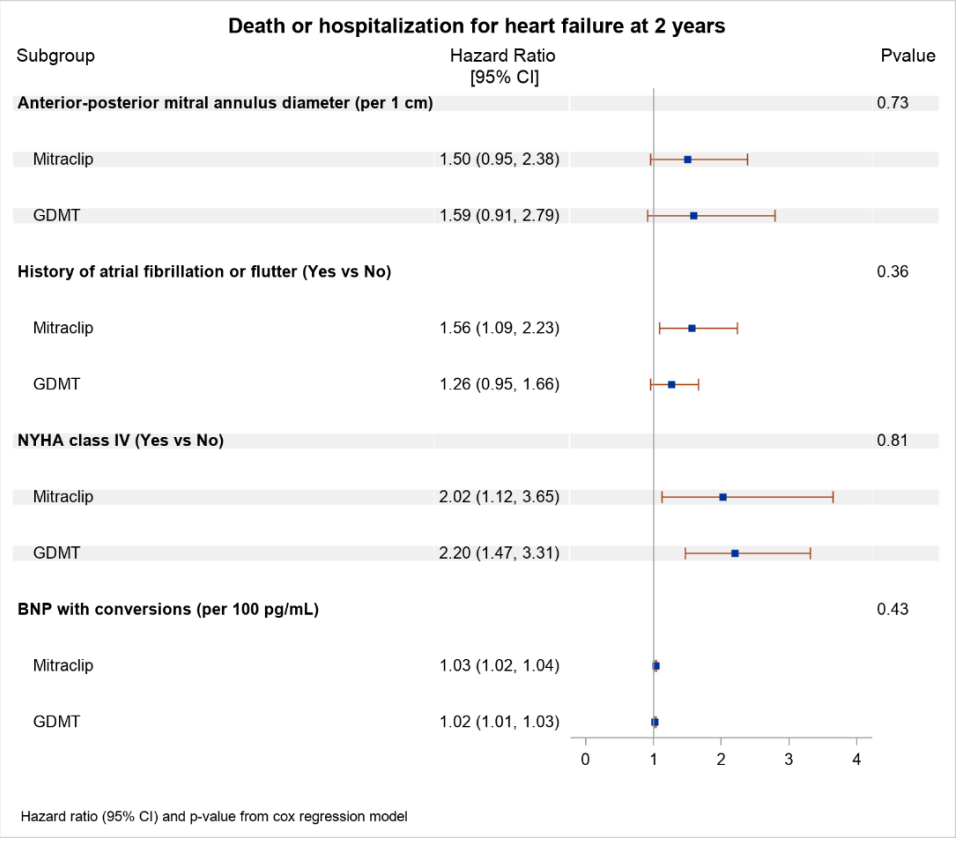

Panel A

Panel B

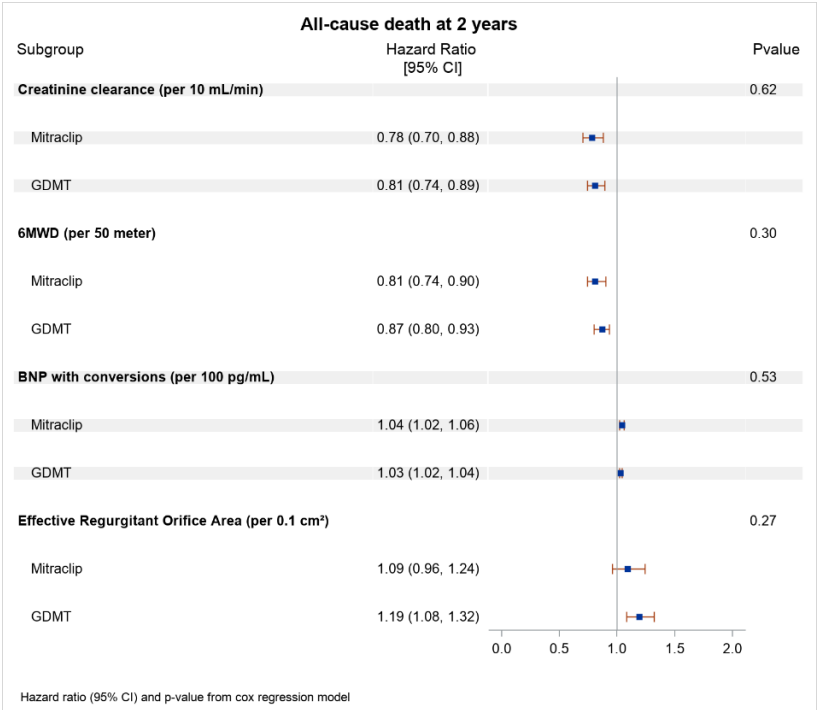

Panel C

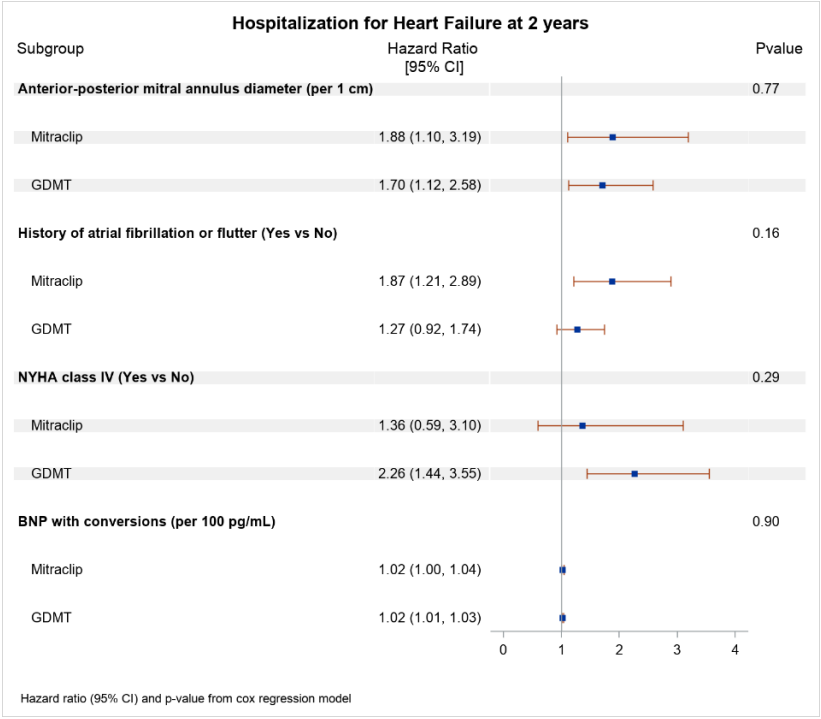

Mitral valve geometry, MR severity and clinical outcomes

LV remodeling in patients with ischemic and non-ischemic cardiomyopathy causes tethering of the mitral valve leaflets and reduced mitral valve closing forces (23). Specifically, global and regional LV remodeling results in increased LV sphericity, papillary muscle displacement, mitral annular dilation and planar flattening. Mitral valve closing forces are reduced due to impaired LV contractility, LV dyssynchrony and reduced mitral annular contraction. The deleterious effects of mitral leaflet tethering and impaired mitral valve closing force leads to lack of leaflet coaptation. The deformation of the mitral valve apparatus may vary greatly depending on the extent of LV remodeling and dysfunction (24). How the various alterations of the mitral valve geometry influence the outcomes of HF patients treated with MitraClip compared with GDMT alone has not been extensively investigated. Mantegazza et al showed that a severely enlarged anteroposterior mitral annular diameter (≥4.44 cm) was associated with significant residual MR after MitraClip implantation, but the authors did not report its effect on outcomes (25). The present substudy from the COAPT trial provides novel evidence by demonstrating an independent association between increasing anteroposterior mitral annular dilation and the composite 2-year outcome of all-cause mortality and HFH, and with the endpoint of HFH alone. Moreover, these associations were similar in both treatment arms suggesting that MitraClip plus GDMT will improve the relative prognosis across the range of anteroposterior mitral annular diameters enrolled within the COAPT trial, with the absolute benefits being greater with larger anteroposterior diameters.

Quantitative measures of MR severity (such as the EROA) have been associated with impaired outcomes. In secondary MR, an EROA >0.2 cm^2 has been associated with poor survival (19). However, randomized controlled trials have shown that surgical or TMVr techniques in patients with secondary MR have a prognostic benefit when the EROA (as a measure of MR severity) is at least 0.3 cm^2 (13,14,26).

In the COAPT trial, in which the vast majority of patients had a baseline EROA ^{3}0.3 cm^2,(15) an increasing EROA was independently associated with increased risk of all-cause mortality alone but not with HFH. MitraClip reduced mortality to a similar relative degree regardless of baseline EROA; as such, the absolute reduction of mortality was greater in patients with greater severity baseline MR treated with the MitraClip.

Grayburn, Packer and colleagues have ventured that the MitraClip is especially likely to improve event-free survival in patients with secondary MR with an EROA that is disproportionate to the extent of LV remodeling (8). Many patients with proportionate

MR are also likely to benefit from MR reduction. In contrast, patients with very advanced LV remodeling and marked dilatation may not respond to MR reduction with the MitraClip, even if the baseline EROA is abnormal. In COAPT, enrollment was strictly controlled to require 3+ or 4+ secondary MR (confirmed by a echocardiographic core laboratory prior to randomization), and LV dimensions were restricted by requiring a LV end-systolic diameter of <7 cm. This requirement likely limited the degree of mitral annular dilatation present in the patients enrolled. Whether the MitraClip would be effective if used in patients with greater LV remodeling and anteroposterior mitral annular diameters than studied with COAPT cannot be addressed by this study. Moreover, whether therapies such as mitral valve annuloplasty may be of greater benefit than the MitraClip or further improve outcomes if used in combination with the MitraClip when the mitral annulus is dilated deserves further study. Similarly, identifying when LV dilatation and mitral annular diameters are too abnormal to benefit from the MitraClip (or other therapies aimed at reducing secondary MR) is essential for optimal patient triage to transcatheter mitral valve repair or replacement versus an LV assist device or heart transplantation.

Predictors of mitral regurgitation reduction after MitraClip

Procedural success rates with the MitraClip have steadily improved with increasing operator experience and advanced imaging guidance. In the present trial 92.3% of MitraClip-treated patients achieved a reduction in baseline MR grade of 3+ or 4+ to <2+ at 30 days. Residual secondary MR ^{3}3+ has not surprisingly been shown in COAPT and other studies to be strongly associated with subsequent adverse events (27-30). In a study of 300 patients with secondary MR undergoing MitraClip treatment, the EROA, mitral valve orifice area (MVOA), and transmitral pressure gradient were associated with inadequate MR reduction (28). The early EVEREST II trial also excluded patients with LV end-systolic dimension >55 mm, MVOA <4.0 cm^{2}, and those with secondary MR and advanced tethering with either coaptation depth >11 mm or vertical coaptation length <2 mm (31). In contrast, COAPT excluded patients with degenerative mitral valve disease, LV end-systolic dimension >70 mm, MVOA <4.0 cm^{2} and those who in the opinion of the site operator had leaflet anatomy that may preclude MitraClip implantation, proper positioning or sufficient reduction in MR; specific anatomic exclusion criteria were not otherwise provided (11). Among patients meeting the enrollment criteria, we identified MR severity 4+ rather than 3+ (but not EROA), tethering location (especially P3), greater mitral posterior leaflet angle, stroke volume, LV end-diastolic volume index and RVSP as predictors of greater residual MR after MitraClip implantation. Further analyses are underway to characterize the mechanisms and implications of these observations.

Limitations

As a post hoc analysis the present results should be considered exploratory and hypothesis generating. The potential impact of unmeasured confounders cannot be excluded; thus, demonstrating associations in multivariable analysis does not prove causality. The operators participating in COAPT in general were very experienced; similar results may not be achieved by operators who have not yet traversed the learning curve (32). Not all echocardiographic parameters of interest were assessed in the present study, and additional insights might have been gained by 3D echocardiographic assessment (33). Finally, by protocol patients with marked LV dysfunction were excluded, some pathologies (e.g. P3 tethering) were infrequently present, and of course the results apply solely to treatment of functional MR. Further studies are thus warranted to examine the prognostic implications of mitral valve anatomies not included in the present study.

Conclusions

In the present echocardiographic core laboratory study from the multicenter COAPT trial, among HF patients with 3+ or 4+ secondary MR, a large anteroposterior mitral annular diameter was associated with increased risk of the composite outcome of all-cause death or HFH and HFH alone. Greater EROA was an independent predictor of mortality. Treatment with the MitraClip plus GDMT compared with GDMT lone reduced death and HFH consistently in patients with and without these extremes.

References

1. Baumgartner H, Falk V, Bax JJ et al. 2017 ESC/EACTS Guidelines for the management of valvular heart disease. Eur Heart J 2017;38:2739-2791.
2. Nishimura RA, Otto CM, Bonow RO et al. 2017 AHA/ACC Focused Update of the 2014 AHA/ACC Guideline for the Management of Patients With Valvular Heart Disease: A Report of the American College of Cardiology/American Heart Association Task Force on Clinical Practice Guidelines. Circulation 2017;135:e1159-e1195.
3. Ponikowski P, Voors AA, Anker SD et al. 2016 ESC Guidelines for the diagnosis and treatment of acute and chronic heart failure: The Task Force for the diagnosis and treatment of acute and chronic heart failure of the European Society of Cardiology (ESC)Developed with the special contribution of the Heart Failure Association (HFA) of the ESC. Eur Heart J 2016;37:2129-2200.
4. Yancy CW, Jessup M, Bozkurt B et al. 2017 ACC/AHA/HFSA Focused Update of the 2013 ACCF/AHA Guideline for the Management of Heart Failure: A Report of the American College of Cardiology/American Heart Association Task Force on Clinical Practice Guidelines and the Heart Failure Society of America. J Am Coll Cardiol 2017;70:776-803.
5. van der Bijl P, Khidir M, Ajmone Marsan N et al. Effect of Functional Mitral Regurgitation on Outcome in Patients Receiving Cardiac Resynchronization Therapy for Heart Failure. Am J Cardiol 2019;123:75-83.
6. Ypenburg C, Lancellotti P, Tops LF et al. Acute effects of initiation and withdrawal of cardiac resynchronization therapy on papillary muscle dyssynchrony and mitral regurgitation. J Am Coll Cardiol 2007;50:2071-7.
7. Gaasch WH, Meyer TE. Secondary mitral regurgitation (part 2): deliberations on mitral surgery and transcatheter repair. Heart 2018;104:639-643.
8. Packer M, Grayburn PA. Contrasting Effects of Pharmacological, Procedural, and Surgical Interventions on Proportionate and Disproportionate Functional Mitral Regurgitation in Chronic Heart Failure. Circulation 2019;140:779-789.
9. Ciarka A, Braun J, Delgado V et al. Predictors of mitral regurgitation recurrence in patients with heart failure undergoing mitral valve annuloplasty. Am J Cardiol 2010;106:395-401.
10. Magne J, Pibarot P, Dagenais F, Hachicha Z, Dumesnil JG, Senechal M. Preoperative posterior leaflet angle accurately predicts outcome after restrictive mitral valve annuloplasty for ischemic mitral regurgi-

tation. Circulation 2007;115:782-91.
11. Van Mieghem NM, Piazza N, Anderson RH et al. Anatomy of the mitral valvular complex and its implications for transcatheter interventions for mitral regurgitation. J Am Coll Cardiol. 2010 Aug 17;56(8):617-26.
12. Wunderlich NC, Siegel RJ. Peri-interventional echo assessment for the MitraClip procedure. Eur Heart J Cardiovasc Imaging. 2013 Oct;14(10):935-49.
13. Stone GW, Lindenfeld J, Abraham WT et al. Transcatheter Mitral-Valve Repair in Patients with Heart Failure. N Engl J Med 2018;379:2307-2318.
14. Obadia JF, Messika-Zeitoun D, Leurent G et al. Percutaneous Repair or Medical Treatment for Secondary Mitral Regurgitation. N Engl J Med 2018;379:2297-2306.
15. Mack MJ, Abraham WT, Lindenfeld J et al. Cardiovascular Outcomes Assessment of the MitraClip in Patients with Heart Failure and Secondary Mitral Regurgitation: Design and rationale of the COAPT trial. Am Heart J 2018;205:1-11.
16. Asch FM, Grayburn PA, Siegel RJ et al. Echocardiographic Outcomes After Transcatheter Leaflet Approximation in Patients With Secondary Mitral Regurgitation: The COAPT Trial. J Am Coll Cardiol. 2019 Dec 17;74(24):2969-2979.
17. Lang RM, Badano LP, Mor-Avi V et al. Recommendations for cardiac chamber quantification by echocardiography in adults: an update from the American Society of Echocardiography and the European Association of Cardiovascular Imaging. Eur Heart J Cardiovasc Imaging 2015;16:233-70.
18. Rudski LG, Lai WW, Afilalo J et al. Guidelines for the echocardiographic assessment of the right heart in adults: a report from the American Society of Echocardiography endorsed by the European Association of Echocardiography, a registered branch of the European Society of Cardiology, and the Canadian Society of Echocardiography. J Am Soc Echocardiogr 2010;23:685-713; quiz 786-8.
19. Zoghbi WA, Adams D, Bonow RO et al. Recommendations for Noninvasive Evaluation of Native Valvular Regurgitation: A Report from the American Society of Echocardiography Developed in Collaboration with the Society for Cardiovascular Magnetic Resonance. J Am Soc Echocardiogr 2017;30:303-371.
20. Lancellotti P, Moura L, Pierard LA et al. European Association of Echocardiography recommendations for the assessment of valvular regurgitation. Part 2: mitral and tricuspid regurgitation (native valve disease). Eur J Echocardiogr 2010;11:307-32.
18. Lancellotti P, Tribouilloy C, Hagendorff A et al. Recommendations for the echocardiographic assessment of native valvular regurgitation: an

executive summary from the European Association of Cardiovascular Imaging. Eur Heart J Cardiovasc Imaging 2013;14:611-44.

19. Otsuji Y, Kumanohoso T, Yoshifuku S et al. Isolated annular dilation does not usually cause important functional mitral regurgitation: comparison between patients with lone atrial fibrillation and those with idiopathic or ischemic cardiomyopathy. J Am Coll Cardiol 2002;39:1651-6.
23. Bertrand PB, Schwammenthal E, Levine RA, Vandervoort PM. Exercise Dynamics in Secondary Mitral Regurgitation: Pathophysiology and Therapeutic Implications. Circulation 2017;135:297-314.
21. Agricola E, Oppizzi M, Maisano F et al. Echocardiographic classification of chronic ischemic mitral regurgitation caused by restricted motion according to tethering pattern. Eur J Echocardiogr 2004;5:326-34.
22. Mantegazza V, Pasquini A, Agati L et al. Comprehensive Assessment of Mitral Valve Geometry and Cardiac Remodeling With 3-Dimensional Echocardiography After Percutaneous Mitral Valve Repair. Am J Cardiol 2018;122:1195-1203.
26. Michler RE, Smith PK, Parides MK et al. Two-Year Outcomes of Surgical Treatment of Moderate Ischemic Mitral Regurgitation. N Engl J Med 2016;374:1932-41.
27. Grayburn PA, Sannino A, Cohen DJ et al. Predictors of Clinical Response to Transcatheter Reduction of Secondary Mitral Regurgitation: The COAPT Trial. J Am Coll Cardiol. 2020 Sep 1;76(9):1007-1014.
28. Lubos E, Schluter M, Vettorazzi E et al. MitraClip therapy in surgical high-risk patients: identification of echocardiographic variables affecting acute procedural outcome. JACC Cardiovasc Interv 2014;7:394-402.
29. Reichart D, Kalbacher D, Rübsamen N et al. The impact of residual mitral regurgitation after MitraClip therapy in functional mitral regurgitation. Eur J Heart Fail 2020;22:1840-1848.
30. Tabata N, Weber M, Sugiura A et al. Impact of the Leaflet-to-Annulus Index on Residual Mitral Regurgitation in Patients Undergoing Edge-to-Edge Mitral Repair. JACC Cardiovasc Interv 2019;12:2462-2472.
31. Feldman T, Foster E, Glower DD et al. Percutaneous repair or surgery for mitral regurgitation. N Engl J Med. 2011 Apr 14;364(15):1395-406.
32. Chhatriwalla AK, Vemulapalli S, Szerlip M et al. Operator Experience and Outcomes of Transcatheter Mitral Valve Repair in the United States. J Am Coll Cardiol. 2019 Dec 17;74(24):2955-2965.
33. Faletra FF, Pedrazzini G, Pasotti E et al. Role of real-time three dimensional transoesophageal echocardiography as guidance imaging modality during catheter based edge-to-edge mitral valve repair. Heart 2013;99:1204-15.